CrossMark

ORIGINAL ARTICLE

EEMD-based online milling chatter detection by fractal dimension and power spectral entropy

Yongjian Ji[1] · Xibin Wang[1] · Zhibing Liu[1] · Zhenghu Yan[1] · Li Jiao[1] ·
Dongqian Wang[1] · Junqing Wang[1]

Abstract Chatter is a kind of self-excited unstable vibration during machining process, which always leads to multiple negative effects such as poor surface quality, dimension accuracy error, excessive noise, and tool wear. For purposes of monitoring the processing state of milling process and detecting chatter timely, a novel online chatter detection method was proposed. In the proposed method, the acceleration signals acquired by sensor were decomposed into a series of intrinsic mode functions (IMFs) by the adaptive analysis method named ensemble empirical mode decomposition (EEMD), and the IMFs which contain the feature information of milling process were selected as the analyzed signals. The two indicators power spectral entropy and fractal dimension which is obtained by morphological covering method are introduced to detect the chatter features. Then, both the frequency characteristic and morphological feature of the extracted signals can be reflected by the two indicators. To verify the approach, milling experiments were performed; the experiment results show that the proposed method can detect chatter timely and effectively, which is important in the aspect of improving the milling quality. And finally, in order to detect milling chatter timely, an online milling chatter monitoring system was developed.

Keywords Milling · Chatter detection · Ensemble empirical mode decomposition · Power spectral entropy · Fractal dimension

✉ Zhibing Liu
liuzhibing@bit.edu.cn

[1] Key Laboratory of Fundamental Science for Advanced Machining, Beijing Institute of Technology, No.5 South Zhongguancun Street, Haidian District, Beijing 100081, People's Republic of China

1 Introduction

Chatter is a self-excited vibration, and it always lead to negative effects on the productivity. Especially in the process of micromilling, the poor surface quality and dimension accuracy error which caused by chatter are fatal defect. Therefore, the avoidance of chatter in milling process has attracted many experts' attention.

Chatter frequencies are very complicated in practice, which are caused by regenerative chatter, frictional chatter [1], thermomechanical chatter [2], mode coupling chatter [3], etc. As discussed by Quintana et al. [4], regenerative chatter is the most common form of self-excited vibration. As shown in Fig. 1, the cutter vibrations leave a wavy surface; when milling, the next tooth in cut attacks this wavy surface and generates a new wavy surface. The chip thickness and the force on the cutting tool vary due to the phase difference between the wave left by the previous teeth and the wave left by the current ones; this phenomenon will help enlarge vibrations, leading to chatter eventually.

In general, the strategies for avoiding chatter are divided into two categories: one is to select proper machining parameters (such as depth of cut and cutting speeds) to change the mechanical system's dynamic behavior [4]; another is the real-time online monitoring the cutting states and adjusting cutting parameters once chatter is about to happen.

The method of selecting right cutting parameters for avoiding chatter is usually based on the stability lobe diagram (SLD). For the purpose of obtaining a reliable SLD, an accurate dynamic model of milling process is necessary, and at present, most of the milling stability analysis methods are based on the classical dynamic control equation [6–8]. Specialists and scholars have proposed many analytic methods for stability analysis of milling processes from the frequency domain [5, 9–13] and time domain [14–19].
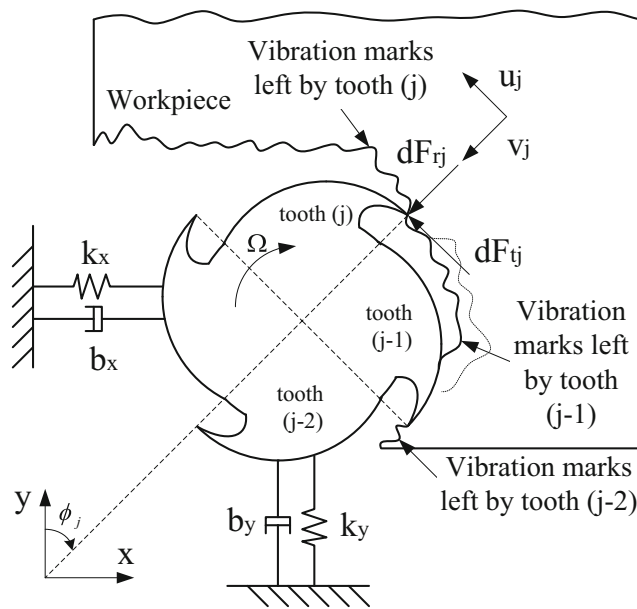
Fig. 1 Regeneration of waviness in a milling model with two degrees of freedom. Source:[5]

Because of the tight coupling and time-varying properties of the whole cutting system, analytic method still could not identically model the real cutting system and perfectly prevent the occurrence of chatter [4, 20]. Therefore, the online signal-based cutting state monitoring and chatter detection methods are very important for practical milling processes to ensure the safety of the machining system and the workpiece [21].

Various signals can be applied to the field of chatter identification, such as acceleration signal [22], sound [23], cutting force [24, 25], torque signal [26], motor current [27], and instantaneous angular speeds [21]. Based on the signals above, many chatter detection methods have been employed in time domain, frequency domain, and time-frequency domain.

Chatter is a complex self-excited vibration, and the chatter signal is nonlinear and nonstationary. Effective signal analysis method is the foundation of chatter identification. Fourier transform has provided a general method for analyzing signals from time domain to frequency domain and has achieved unprecedented success for signals generated by linear and stationary processes. But Fourier transform is not so impressive in terms of processing nonlinear and nonstationary signal. There are also methods for nonlinear and nonstationary signals such as windowed Fourier transform [28], wavelet transform [29], and the Wigner-Ville distribution [30, 31]. However, almost all of the methods above have their own limitations. For example, windowed Fourier transform is based on traditional Fourier analysis, so it is still remains challenges in processing nonlinear and nonstationary signals. When wavelet method is involved, experts will always be needed to set and adjust those model parameters [32].

Empirical mode decomposition (EMD) is a self-adaptive signal analysis method proposed by Huang et al. [33]. EMD has big advantages over the traditional linear method in analyzing nonlinear and nonstationary signals since it is highly adaptive in processing signal. But this method also has some limitations. One of the major drawbacks of EMD is mode mixing. Mode mixing, which is defined as either a single intrinsic mode function (IMF), consists of signals of widely disparate scales or a signal of a similar scale residing in different IMF components; it could not only cause serious aliasing in the time-frequency distribution but could also make the individual IMF lose its physical meaning. Another side effect of mode mixing is the lack of physical uniqueness [34]. In order to overcome the drawbacks of mode mixing, Huang and Wu [35] proposed a noise-assisted method which is called ensemble empirical mode decomposition (EEMD). This method performs well in the aspect of suppressing mode mixing. EEMD has been applied in many scientific fields such as wind energy [36, 37], economy [38], and fault diagnosis [39–42].

A good evaluation indicator is necessary in the aspect of chatter detection. Chatter is a phenomenon reflecting changes of frequency and energy distribution in machining process [43]. So, the nonlinear dimensionless indicators which can reflect the changes of frequency and energy distribution can be applied to judge the severe degree of chatter.

Liu et al. [27] applied standard deviation and energy ratio to identify chatter, but both of the two indicators just can reflect the changes of energy distribution, and it is difficult to the reflect the changes of frequency. In addition, with the increase of cutting thickness, signal energy will also increase; it easily causes misjudgment only according to the change of energy to identify chatter.

The entropy [44] is a function of the probability distribution function. The concept of power spectral entropy (PSE) is the extension of Shannon entropy in frequency domain, and it can reflect the changes of frequency. Power spectral entropy is a good indicator in the aspect of chatter detection.

Fractal theory [45, 46] is proposed by Mandelbrot. Fractals are virtual geometrical objects that appear identical regardless of the length scale, which can be characterized by a single parameter—fractal dimension (FD) [47]. Fractal dimension plays an important role in the aspect of texture segmentation [48], shape classification [49], and graphic analysis [50]. The typical methods of calculating fractal dimension can be divided into four categories: the box counting method [51], the variance methods, the spectral methods, and the morphological covering method [52]. The morphological covering method is more robust than the box counting method when dealing with discrete signals, because it can yield results that are

invariant with respect to shifting the signal's domain or affine scaling of its dynamic range. What is more, this method is more effective in terms of processing one-dimensional signal.

Chatter is a phenomenon of reflecting changes of frequency and energy distribution in machining process. In addition, the structure of the captured signal is also changed when chatter occurs. An indicator that both can reflect these characteristics is necessary in the aspect of detecting chatter. But in fact, it is difficult to find such an indicator. On the other hand, only according to the change of energy to identify chatter is not reliable. As discussed by Cao [53], in the stable cutting case, the frequency components are evenly distributed in all frequency ranges, and the morphology of the signal is relatively regular. As the chatter severity level increases, the frequency components gradually gather at the location of chatter frequencies, and the morphology of the signal is disordered. Power spectral entropy can reflect the changes of frequencies; however, it is difficult to indicate the changes of the signal morphology. The fractal dimension obtained by the morphological covering method is an important characteristic of fractals that contains information about their geometrical structure at multiple scales. So, it can reflect the change of signal morphology.

Based on the analysis above, a novel online milling chatter detection method is proposed. The EEMD method is presented as a preprocessing tool for the measured signals. The PSE and FD which is obtained by the morphological covering method are applied to identify the chatter state. In order to obtain the information which can reflect milling state to the greatest extent, the following chatter analysis method is based on the acceleration signal. The originality of the proposed method is that the original characteristic information is extracted by EEMD method firstly, and then, both of the frequency characteristic and morphological features of the extracted signals are reflected by power spectral entropy and fractal dimension; it means that the milling chatter can be detected from different aspects. Therefore, the diagnosis result is more reliable. In other words, misjudgment can be avoided when assessing the milling state by considering the two indicators. On the other hand, it is more convenient to judge different milling states by the specific values, i.e., the values of power spectral entropy and fractal dimension.

The organization of this paper is as follows: brief introduction of EMD, EEMD, FD, and PSE are given in Sect. 2. Section 3 introduces the proposed chatter identification method, including the experimental setup, the feature extraction of chatter, the determination of chatter threshold, and the validation of the chatter identification method. The online chatter monitoring strategy is proposed in Sect. 4. The realization of the online milling chatter monitoring is given in Sect. 5. Finally, the conclusions and future works are laid out in Sect. 6.

2 Introduction of ensemble empirical mode decomposition, fractal dimension, and power spectral entropy

2.1 Empirical mode decomposition and the ensemble empirical mode decomposition

The EMD method is a new adaptive signal decomposition method, and it has big advantages over the traditional linear method in analyzing nonlinear and nonstationary signals since it is highly adaptive in processing signal. This method can decompose a nonlinear, nonstationary time series into several components referred to as IMFs. an IMF should satisfies two conditions [33]: (1) in the whole dataset, the number of extrema and the number of zero crossings must either equal or differ at most by one; (2) at any point, the mean value of the envelope defined by the local maxima and the envelope defined by the local minima is zero. However, one of limitations of EMD is mode mixing, which could not only cause serious aliasing in the time-frequency distribution but could also make the individual IMF loses its physical meaning. Another side effect of mode mixing is the lack of physical uniqueness [34]. The EEMD [35] method is a noise-assisted method EMD which proposed by Wu and Huang, utilizing the full advantage of the Gaussian white noise's statistical characteristic of uniform distribution to improve the distribution of extreme points in original signal; this method performers well in the aspect of solving the problem of mode mixing.

The basic idea of EEMD is that the signals are combined with the true time series and noise. Thus, if data are collected by separate observations, each with a different noise level, the ensemble mean is close to the true time series. Therefore, an additional step is taken by adding white noise that may help extract the true signal in the data. The effect of the added white noise can be controlled by the well-established statistical rule, calculated as in Eq. 1.

$$\varepsilon_n = \frac{\varepsilon}{\sqrt{N}} \qquad (1)$$

where N is the number of ensemble members, ε is the amplitude of the added noise, and ε_n is the final standard deviation of error, defined as the difference between the input signal and the corresponding IMFs. In practice, the number of ensemble members is often set to 100 and the standard deviation of white noise series is set to 0.1 or 0.2 [38].

2.2 Fractal dimension obtained by the morphological covering method

Fractals can model many classes of time-series data. The FD is an important characteristic of fractals that contains

information about their geometrical structure at multiple scales. The covering methods are a class of efficient approaches to measure the fractal dimension of an arbitrary fractal signal by creating multiscale covers around the signal's graph. The steps of calculating the FD of a discrete-time finite-length signal $f(t)$, $t = 1, 2, ..., N$ by the morphological covering method are expressed as follows [52]:

1. Select a set structuring element B. B is a compact planar set and B should be a convex symmetric subset of the 3×3 square set of points from the rectangular grid of pixels (n, mh), where (n, m) are integer coordinates and h is the vertical grid spacing. Then, $g[n]$, $n = -1, 0, 1$, is a three-sample function whose graph is the upper envelope of B. There are only three choices for such a unit-radius B: the 3×3-pixel square, the 5-pixel rhombus, and the 3-pixel horizontal segment. If B is the 3×3-pixel square, the corresponding g is shaped like a rectangle, that is $g_r[-1] = g_r[0] = g_r[1] = h \geq 0$ and $g_r[n] = -\infty$ for $n \neq -1, 0, 1$. If B is the 5-pixel rhombus, then g is shaped like a triangle, defined by $g_t[-1] = g_t[1] = 0$, $g_t[0] = h \geq 0$, and $g_t[n] = -\infty$ for $n \neq -1, 0, 1$. If B is the 3-pixel horizontal segment, then the corresponding g can be regarded as resulting either from g_t or g_r by setting $h = 0$.

2. Perform recursively the support-limited dilations $\oplus$ and erosions Θ of $f(t)$ by $g^{\oplus \varepsilon}$ at scales $\varepsilon = 1, 2, 3, ..., \varepsilon_{max}$, yield

$$\begin{cases} f \oplus sg[n] = \max_{-1 \leq i \leq 1} \{f[n+i] + g[i]\}, \varepsilon = 1 \\ f \oplus sg^{\oplus(\varepsilon+1)} = (f \oplus sg^{\oplus\varepsilon}) \oplus sg, \varepsilon \geq 2 \end{cases} \quad (2)$$

where s is a support set and $S = \{0, 1, 2, ..., N\}$, and N denotes the length of signal $f(t)$.

$$f \oplus sg^{\oplus\varepsilon} = \underbrace{((f \oplus sg) \oplus sg...) \oplus sg}_{\varepsilon \text{times}}$$

Likewise, for the erosions $f \Theta sg^{\oplus\varepsilon}$. For $n = 0, N$, the local max/min operations take place only over the available samples.

3. Compute the cover areas

$$A_g[\varepsilon] = \sum_{n=0}^{N} ((f \oplus sg^{\oplus\varepsilon}) - (f \Theta sg^{\oplus\varepsilon}))[n],$$
$$\varepsilon = 1, 2, ..., \varepsilon_{max} \leq \frac{N}{2} \quad (3)$$

where $f \Theta sg^{\oplus\varepsilon} = \underbrace{((f \Theta sg) \Theta sg...) \Theta sg}_{\varepsilon \text{times}}$

4. Fit a straight line using least squares to the graph of $\log(A_g[\varepsilon]/(\varepsilon')^2)$ versus $\log(1/\varepsilon')$,

$$\log \frac{A_g[\varepsilon]}{(\varepsilon')^2} \approx D_M \cdot \log\left(1/\varepsilon'\right) + \text{constant} \quad (4)$$

For $\varepsilon' = 2/N, 4/N, ..., \varepsilon'_{max}$, define $\varepsilon' = 2\varepsilon/N$ as the normalized scale, and $2/N \leq \varepsilon' \leq \varepsilon'_{max} \leq 1$, where $\varepsilon'_{max} = 2\varepsilon_{max}/N$.

The approximate estimate of the fractal dimension $D_M(f)$ can be obtained from the slope of the fitted straight line (Eq. 4). The details of the algorithm are introduced in reference [52].

The fractal dimension $D_M(f)$ of the graph of $f(t)$ resulting from the morphological covering method (in both the continuous and discrete case) has the following two attractive properties [48].

1. The fractal dimension $D_M(f)$ will not be changed if f is shifted with respect to its argument or amplitude, that is $D_M(f) = D_M(f')$, where $f'(x) = f(x - x_0) + b$;

2. If $h = 0$, then $D_M(f)$ remains invariant with respect to any affine scaling of the amplitude of $f(t)$ or shifting of its argument.

Because of the two properties above, the morphological covering method is more robust than other methods such as box counting method.

2.3 Power spectral entropy

The concept of power spectral entropy is the extension of Shannon entropy in frequency domain, which is linked to the distribution of frequency components [53]. The power spectral entropy of a given signal is obtained by the following steps [53, 54]:

1. The power spectrum of signal $x(t)$ can be obtained by using Eq. 5.

$$s(f) = \frac{1}{2\pi N} |X(w)|^2 \quad (5)$$

where N is the length of the signal $x(t)$. $X(w)$ is the Fourier transformation of $x(t)$ by the fast Fourier transform (FFT).

2. The probability density function for the spectrum can thus be estimated by normalization over all frequency components:

$$p_i = s(f_i) \bigg/ \sum_{k=1}^{N} s(f_k), i = 1, 2, 3, 4, 5..., N \quad (6)$$

where $s(f_i)$ is the spectral energy of the frequency component f_i, p_i is the corresponding probability density, and N is the total number of frequency components in FFT.

3. The corresponding power spectral entropy is defined as

$$H = -\sum_{k=1}^{N} p_i \cdot \log p_i \qquad (7)$$

For the purpose of comparing different working conditions, the result is normalized by the factor $\log N$, that is

$$E = \frac{H}{\log N} = \frac{-\sum_{k=1}^{N} p_i \cdot \log p_i}{\log N} \qquad (8)$$

The power spectral entropy E is a nondimensional indicator in the range of [0, 1], where 1 corresponds to the spectrum whose distribution of frequency component is comparatively even and uncertain and 0 corresponds to the distribution uncertainty is the least [53].

3 The proposed chatter identification method

The vibration signal is composed of many components. These components not only contain the periodic component due to the rotation of the cutter and intermittent milling of the tool, the chatter vibration component due to regenerative effect, but also contain the stochastic perturbation component due to system noise, inhomogeneous material, etc. [53]. The core problem of chatter identification is to find the frequency components which are related to chatter.

In order to obtain the useful components and remove the noise components and other components which are unrelated to the chatter signals, the EEMD method is applied to decompose the original vibration signal into a series of IMFs; then, the useful IMFs are selected to combine a new signal, and this new signal is the foundation of chatter identification. For the purpose of real-time monitoring the running state of the machine tool and identifying chatter state as soon as possible, the new signal is divided into several segments; then, the FD and PSE of each segment signal are calculated, respectively. Next, the curves based on the fractal dimension and power spectral entropy of each segment are drawn. Furthermore, the distribution chart of the two indicators can be obtained. In the end, the running state of machine tool can be judged according to the change of the fractal dimension curve and power spectral entropy curve or the distribution chart. The flow chart of the proposed chatter identification is illustrated in Fig. 2.
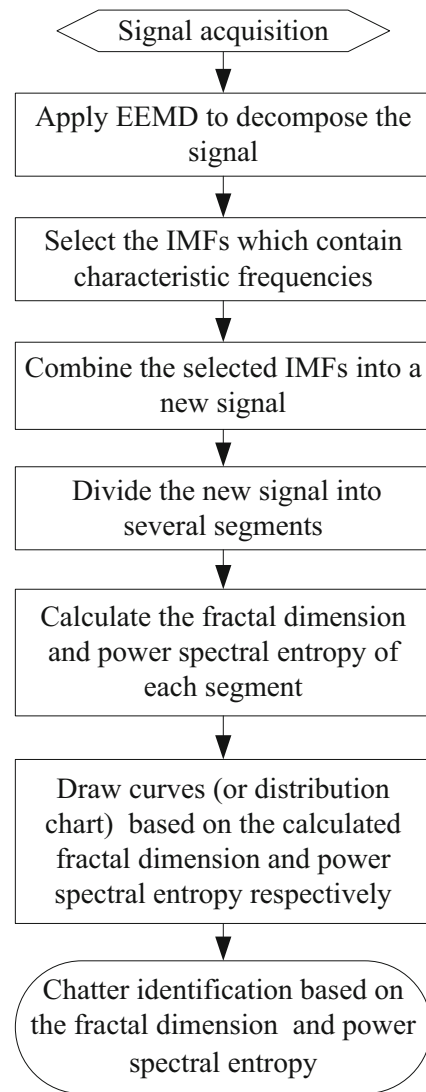

Fig. 2 Flow chart of the proposed method

3.1 Experimental setup

The milling test (side milling) was performed on a high-speed machining center DMU 80. The workpiece material was a block of 2A12 aluminum alloy clamped on the worktable. The cutter was a carbide end mill cutter with four flutes, and its diameter was 10 mm. The accelerometer was mounted on the workpiece to measure the vibration signals during milling process, and the sampling frequency was set as 5120 Hz. The milling condition was dry cutting, downmilling. The experimental schematic diagram is shown in Fig. 3.

Since chatter is closely related to the spindle speed and the depth of cut [6], the experiment was performed with different cutting speed and depth of cut. In order to obtain the vibration signal from stable state to chatter, the SLD, which obtained by the semidiscretization method [55], is applied to determine the approximate cutting parameters. For the purpose of obtaining
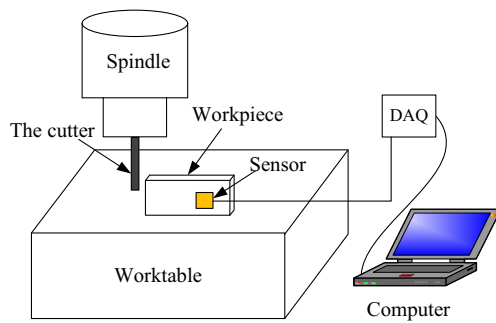
Fig. 3 The experimental schematic diagram

Fig. 4 The modal test experiment

the relative parameters of the SLD, a modal test experiment was carried out firstly.

The modal tests were performed to identify the modal parameters. In the experiments, the cutting tool and workpiece were clamped on the high-speed machining center DMU 80. An INV9822 type acceleration sensor was attached to the selected position on the workpiece in order to obtain response signals. The sensitivity of this acceleration sensor is 10.355 mV/ms^{-2}, and the available frequency range is 0.5–8000 Hz. A MSC-1 impact hammer with a 500 kgf sensor was employed to knock the workpiece with the aim of generating stimulus signals. A DLF-3 type two-channel charge amplifier with an attenuation rate greater than 140 Db/oct was used to amplify the stimulus signals. Finally, the stimulus signals were acquired by an AD8304 type four-channel data acquisition unit and analyzed by DynaCut software. The modal test experiment is shown in Fig. 4. The modal parameters of the tool-workpiece system are listed in Table 1.

In Table 1, f_n denotes the natural frequency, ξ denotes the relative damping, and m_t denotes the modal mass. The tangential cutting force coefficient K_t and the normal linear cutting force coefficient K_n were obtained by experiment, $K_t = 696.8 Mpa$, $K_n = 201.2 Mpa$. The radial depth of cut $a_e = 5$-mm and the diameter of the milling cutter $D = 10$ mm. The milling style is downmilling. So, the tooth entering angle of the workpiece $\phi start = arc \cos(2ae/D - 1) = 1.571$ and the tooth exiting angle $\phi exit = \pi$.

According to the parameters above, the SLD is obtained, as shown in Fig. 5. The SLD distinguishes regions of stable and unstable cutting operation for different combinations of axial depth of cut and spindle speed. Theoretically, when the axial depth of cut and spindle speed are selected under the stability lobes, the cutting process would be stable (chatter-free). Otherwise, the cutting process would be unstable (chatter) [6].

Three kinds of different milling conditions which marked A, B, and C are selected in the milling experiment. According

to Fig. 5, the specific processing parameters of different cutting states are shown in Table 2.

The feed per tooth f_t of each milling condition was set as 0.02 mm, and under condition A, the radial depth was set as 3 mm. And both under conditions B and C, the radial depths were set as 5 mm, respectively. The acceleration signal was sampled by an acceleration sensor.

Figure 6 shows the workpiece quality under the three kinds of milling parameters. It is obvious that under the parameter combination of condition B and condition C, the cutting states are stable; under the parameter combination of condition A, the cutting state is varying from stable to chatter. This experiment indicates that the actual cutting state is not identical to the theoretical analysis of stability lobes. The reason is the tight coupling and time-varying properties of the whole cutting system. So, it also shows that it still has a certain challenges to predict machining states by analytic method.

The vibration signals of the three cutting states are shown in Fig. 7. Since condition A shows that the cutting state is varying from stable to chatter, the following chatter analysis is based on the acceleration signal of condition A.

3.2 Selection of the feature components

For the purpose of obtaining the useful components and remove the noise components of the acceleration signal, the EEMD method is applied to decompose the signal into a series of IMFs. Figure 8 shows the first seven IMFs of the acceleration signal sampled under condition A.
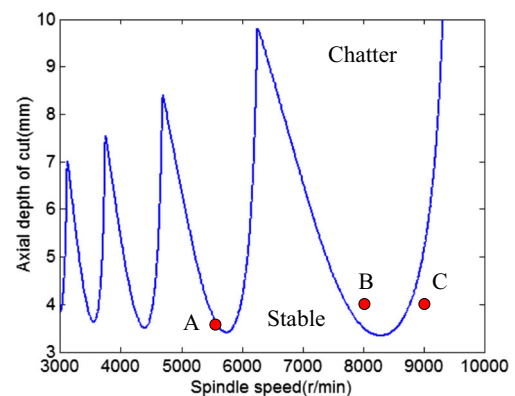

Fig. 5 The stability lobe diagram (SLD)

Table 1 The modal parameters of the tool-workpiece system	f_n (Hz)	ξ(%)	m_t (kg)
	1286.12	0.0289	0.1118

Table 2 The cutting parameters

Cutting condition	Spindle speed n (rpm)	Axial depth of cut a_p (mm)
A	5600	3.5
B	8000	4.0
C	9000	4.0

In order to select sensitive IMFs which contain the main information of milling state, the correlation coefficients and relative energy ratio are introduced to determine the sensitive IMFs. Pseudo-IMF is inevitable during the process of EEMD, and it will bring bad effects to the analysis results. The real IMFs have good correlations with the original signal, but the pseudo-component will not [56]. And usually, the relative energy ratio of the useful IMF is higher than the pseudo. For the purpose of obtaining useful information to the greatest extent, the correlation coefficients between the IMFs and the original signal and the relative energy ratio of each IMF are introduced to choose the real IMFs synchronously.

Figure 9a shows the correlation coefficients between the first seven IMFs and the original signal, and Fig. 9b shows the relative energy ratio of the first seven IMFs to the original signal.

As shown in Fig. 9, the first three IMFs have higher correlation coefficient than others. And also, most of the energy mainly distributes in the first three IMFs. For the purpose of obtaining the useful information and abandoning the useless information, the first three IMFs are selected to combine into a new signal. The following chatter analysis is based on the new signal.

3.3 Chatter detection based on fractal dimension and power spectral entropy

The changing properties of frequency domain can be reflected by the power spectral entropy. In the stable cutting state, the frequencies are evenly distributed in all frequency ranges and it leads the value of power spectral entropy reaches its
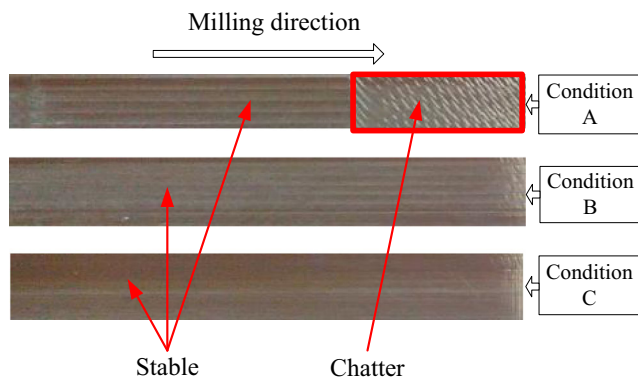

Fig. 6 Workpiece surface under different milling condition
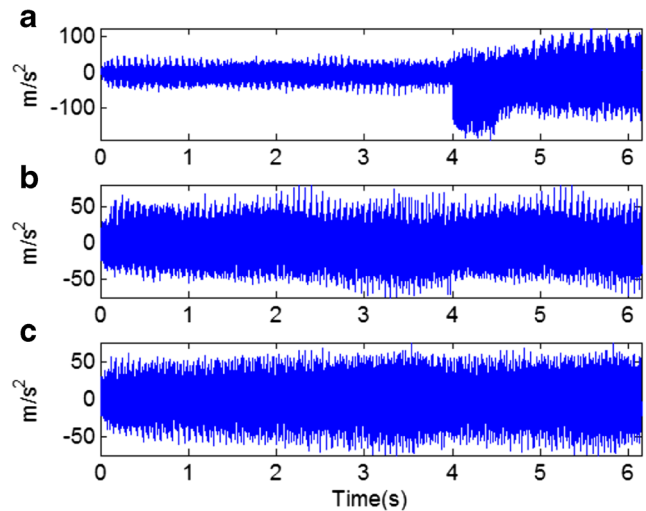

Fig. 7 The acceleration signals of different milling states. **a** Condition A. **b** Condition B. **c** Condition C

maximum. However, when chatter gradually increases, the chatter frequency component plays a leading role in the frequency band, which means that the amplitude of chatter frequencies will gradually increase, and other frequency components can be ignored, which leads to the decreases of the power spectral entropy.

FD can reflect the intrinsic properties of a signal. The fractal dimension obtained by the morphological covering method
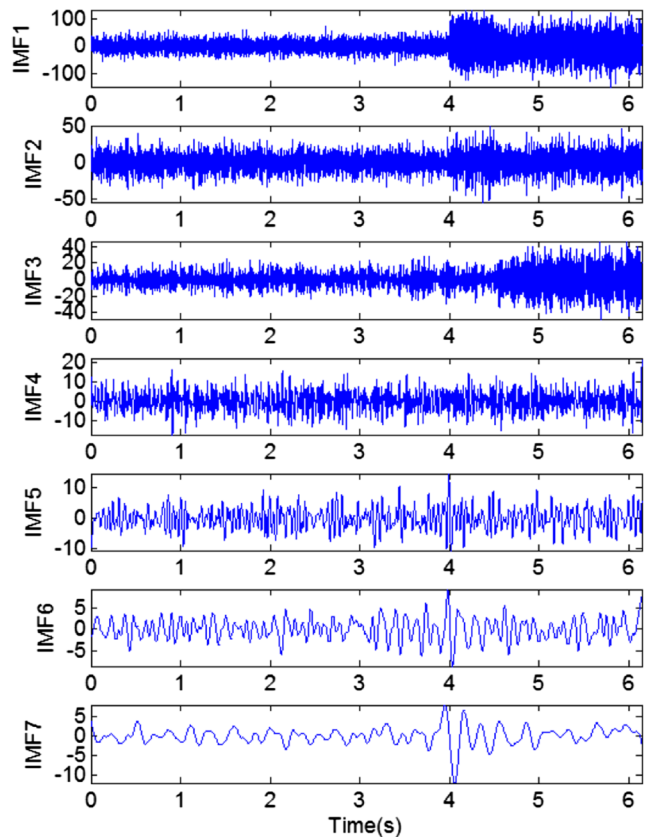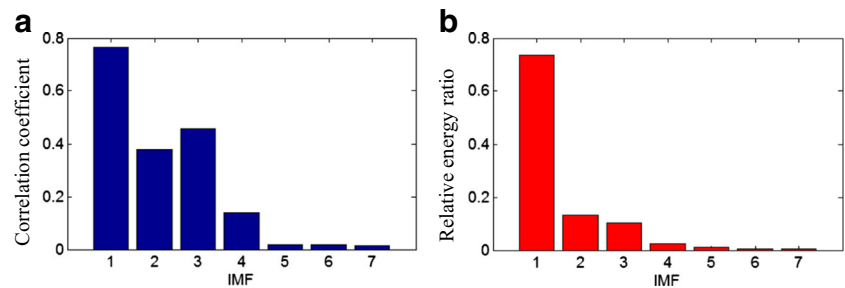

Fig. 8 The first seven IMFs

is a good nondimensional factor of judging chatter. In the stable cutting state, the morphology of the signal is relatively regular, and under this circumstance, the fractal dimension fixed in a relatively small value. However, as the chatter severity level increases, the morphology of the signal is disordered and the value of fractal dimension will increase sharply.

Figure 10 shows the fractal dimension curve and power spectral entropy curve of the acceleration signal under condition A. Figure 10a shows the time-domain signal obtained by the EEMD. Figure 10b shows the fractal dimension curve. Figure 10c shows the power spectral entropy curve. It is clear from Fig. 10a that the amplitude of the signal in the first 4 s is relatively small, but starting from the fifth second, the amplitude of the signal increases dramatically. Since then, the amplitude stable at a relatively high level. It is difficult to judge whether chatter occurs or not according to the time domain signal. Figure 10b shows that in the first 4 s, the value of fractal dimension fluctuates slightly around 1.6; at the beginning of the fifth second, the value of fractal dimension reaches to 1.8 dramatically, which is considerably higher than the value in other areas. However, the fractal dimension falls back to 1.7 starting from the sixth second. Figure 10c shows that in the first 4 s, the value of power spectral entropy close to 0.82; at the beginning of the fifth second, the value of power spectral entropy down to 0.6 suddenly. However, the power spectral

entropy reaches to 0.8 starting from the sixth second. Both of the fractal dimension curve and power spectral entropy curve indicate that chatter occurs in the fifth second; then, it decreases at the beginning of the 4.5 s. Finally, it reached at a new chatter state. In order to validate whether the above analysis is correct or not, the frequency spectrum analysis is applied to analyze the signal.

There are several sources of vibrations in metal cutting processes, and these mechanical vibrations arise due to the lack of dynamic stiffness of one or several elements of the system composed by the machine tool, the tool holder, the cutting tool, and the workpiece material. These vibrations are defined as free vibrations, forced vibrations, and self-excited vibrations. In milling process, the sources of vibrations are also connected to the tooth pass excitation frequency and its higher harmonics [57]. In this article, because some of the low-frequency components have been filtered out by EEMD, there are three main types of frequency components on the frequency band, i.e., chatter frequency, tooth passing frequency, and its harmonics.

Chatter is a self-excited vibration, and chatter frequencies are very complicated in practice, which are caused by regenerative chatter, frictional chatter, thermomechanical chatter, and mode coupling chatter [4]. In this article, the main purpose of using spectrum analysis is to verify the effectiveness of the proposed chatter detection method. The basic principle of
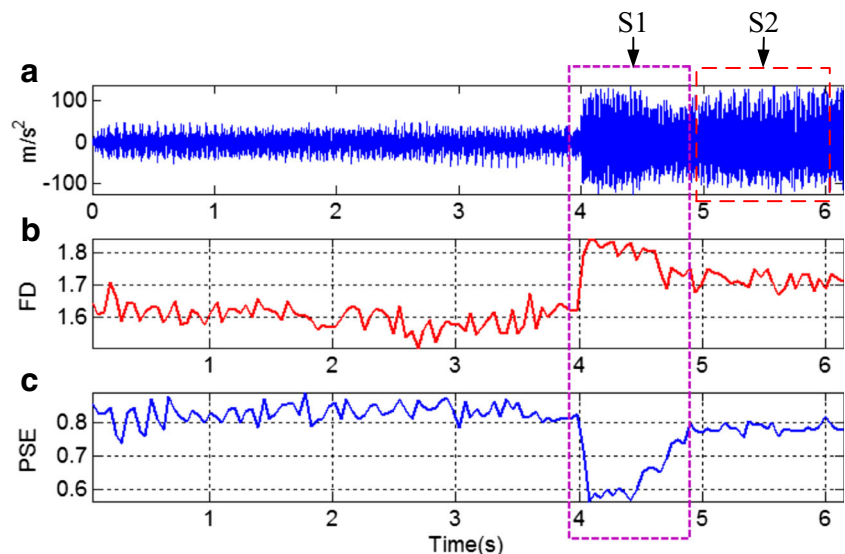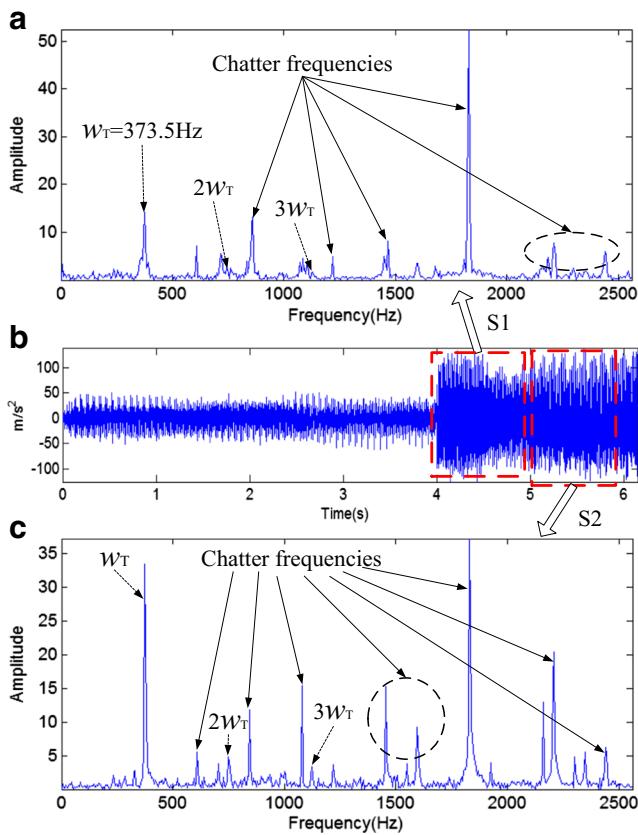
Fig. 11 The frequency spectrum. **a** The frequency spectrum of segment 1 (S1). **b** The acceleration signal selected by EEMD. **c** The frequency spectrum of segment 2 (S2)

detecting chatter by power spectral entropy and fractal dimension is according to the frequency distribution and the morphological structure of the vibration signals; it means that we are more concerned with the frequency distribution and the energy of the chatter frequency when detecting chatter by the two indicators.

Figure 11 shows the frequency spectrum of different time periods. Figure 11a shows the frequency spectrum
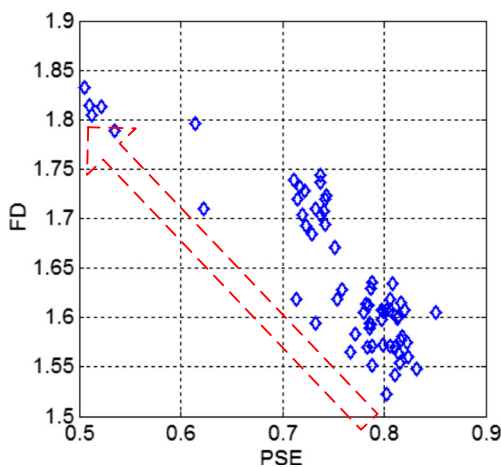
Table 3 The cutting parameters and values of FD and PSE

n (rpm)	f_t (mm)	a_p (mm)	w (mm)	FD	PSE
3500	0.01	3.2	2	1.62	0.81
4000	0.01	3.2	2	1.59	0.83
4500	0.02	3.2	2	1.55	0.85
5000	0.02	3.5	2	1.59	0.82
5500	0.03	2	2	1.62	0.75
6000	0.03	4	3	1.63	0.75
6500	0.04	4	3	1.58	0.77
7000	0.04	4	3	1.65	0.75
7500	0.15	3.5	3	1.57	0.82
8000	0.15	3.2	3	1.60	0.78

of segment 1 (S1); it is clear from Fig. 11a that there are three main types of frequency components, i.e., chatter frequency, tooth passing frequency (w_T), and its harmonics (kw_T) due to periodic tooth pass excitation effect, where k is a positive integer number. And chatter frequency components play a dominant role in the frequency band. Figure 11c shows the frequency spectrum of segment 2 (S2), and although the chatter frequencies also exist in the frequency bands, the amplitude of each chatter frequency is reduced; the tooth passing frequency and its harmonics occupy a large proportion in the frequency band. It indicates that the milling chatter is reduced at the beginning of the sixth second. The analysis result of frequency spectrum is in accordance with the changing trend of fractal dimension curve and power spectral entropy curve. We can come to the conclusion that according to the changes of fractal dimension curve and power spectral entropy curve, the chatter state can be identified accurately.

In order to judge the milling state more intuitive and convenient, the values of fractal dimension and power spectral
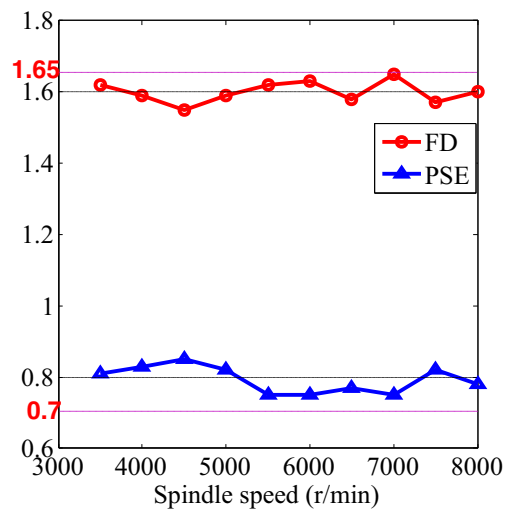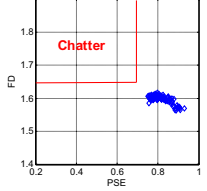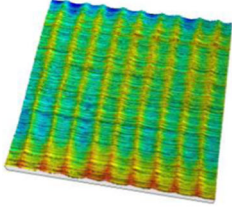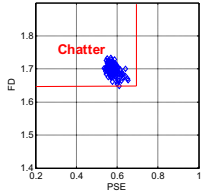

Fig. 12 The distribution chart of fractal dimension and power spectral entropy under different milling states
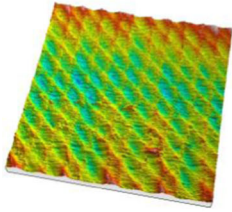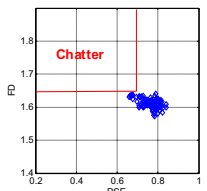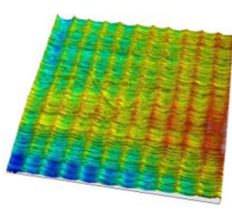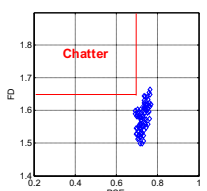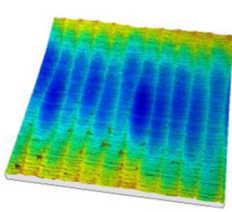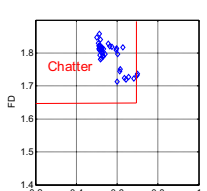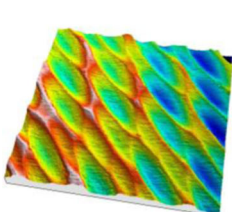
Fig. 13 The values of fractal dimension (FD) and power spectral entropy (PSE) under different milling conditions

Table 4 The cutting parameters and the analysis result of each milling state

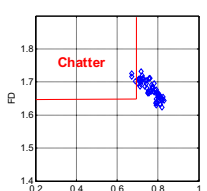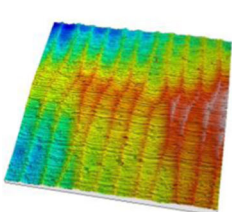| No.	n (rpm)	f_t (mm)	a_p (mm)	w (mm)	The classification chart and the average values of FD and PSE	Surface topography	Surface roughness (μm)	Milling state
1	5000	0.05	4	2	FD=1.6; PSE=0.82		0.295	Stable
2	5500	0.05	4	2	FD=1.69; PSE=0.58		1.558	Slight chatter
3	6000	0.05	4	2	FD=1.60; PSE=0.76		0.365	Stable
4	6500	0.05	4	2	FD=1.58; PSE=0.72		0.850	Stable
5	7000	0.05	5	2	FD=1.67; PSE=0.76		0.872	Stable
6	7500	0.05	5	2	FD=1.80; PSE=0.56		2.867	Severe chatter

Fig. 14 The milling state diagrams (top view)

entropy of condition A are displayed in the same image; then, the distribution chart of the two indicators can be obtained, as shown in Fig. 12.

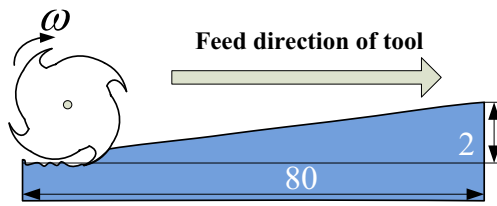According to Fig. 12, we can notice that the values of fractal dimension and power spectral entropy are distributed in different areas, which means different milling states. In the direction of the arrow, the milling state changes from stable to chatter. When the values of the two indicators appear on the top left corner of the image, severe chatter occurs. To determine the chatter area on the image, the thresholds of fractal dimension and power spectral entropy should be determined firstly.
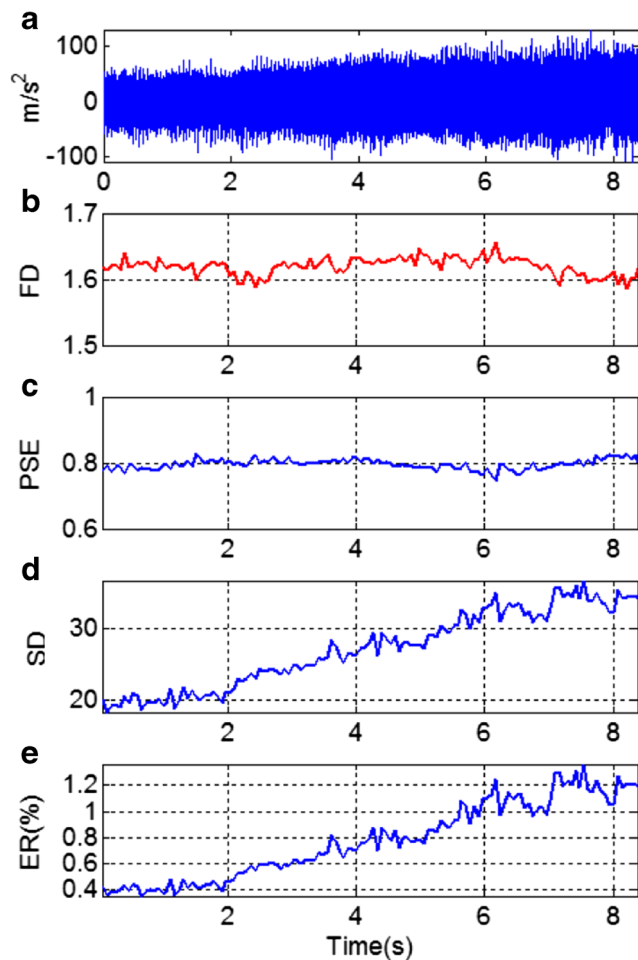

Fig. 15 The acceleration signal and the curves of different indicators

3.4 The determination of chatter threshold

Through the experimental analysis of Sect. 3.3, it is clear that the stable (chatter-free) and chatter states can be identified according to FD and PSE.

In practical milling, to detect chatter accurately, the reliable chatter thresholds (i.e., the stability boundary) with respect to fractal dimension and power spectral entropy are indispensable. Theoretically, in a stable cut, the value of power spectral entropy is relatively high and the value of FD is relatively low. Using a higher power spectral entropy value and a lower fractal dimension value as the thresholds means that the onset is detected sooner, but it increases the possibility of a cut being detected as exhibiting chatter, whereas the workpiece surface quality is still acceptable. However, when using a lower power spectral entropy value and a higher fractal dimension value as the thresholds, it might occur that the cut is exhibiting chatter, i.e., the surface of workpiece is damaged, but it is not detected.

In the paper, to determine the reliable chatter threshold level, milling experiments have been performed to choose the stability boundary. The acceleration signal was also taken as the signal to be studied. The experimental device is the same as Sect. 3.1. The specific processing parameters of different milling states and the values of FD and PSE of each milling state are shown in Table 3. In Table 3, n, f_t, a_p, and w denote the spindle speed, feed per tooth, axial depth of cut, and radial depth, respectively. After testing the quality of the workpiece surface topography [58], we have already known that all of the milling states are stable.
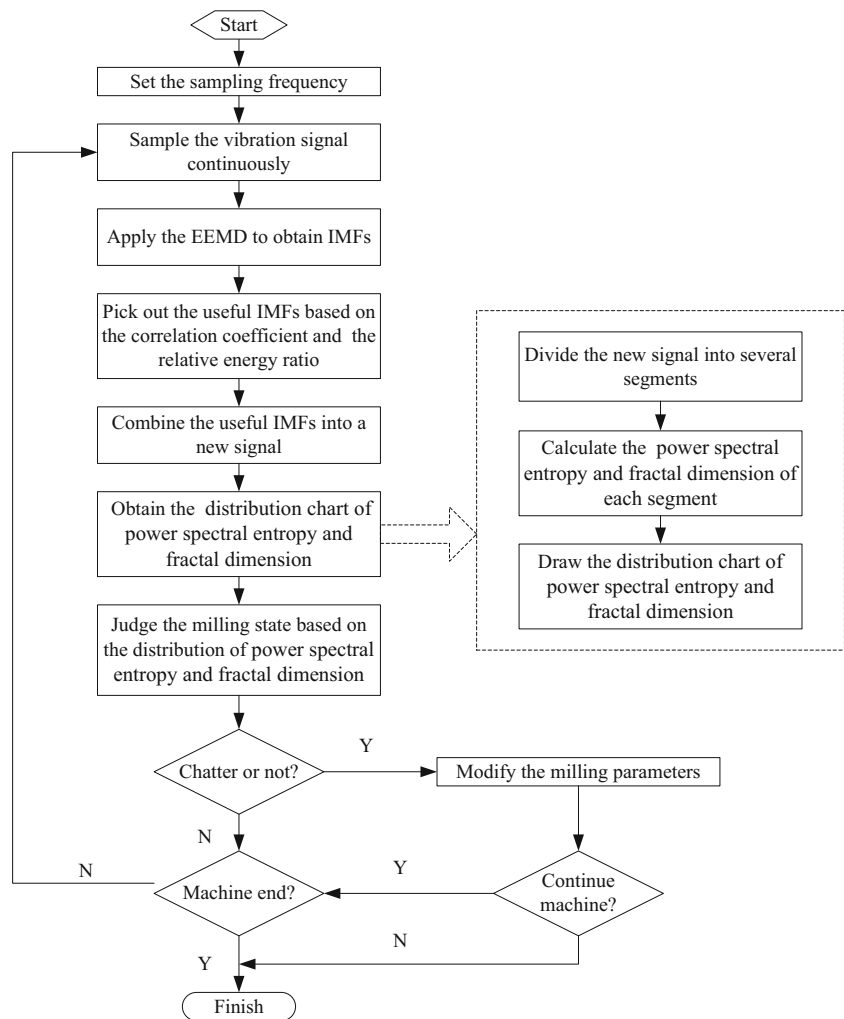
The values of FD and PSE under different milling conditions are shown in Fig. 13. It is clear that all of the values of FD fluctuate around 1.6, and both of them are less than 1.65. Meanwhile, both of the values of PSE are above 0.7. Based on the experimental analysis above, the chatter threshold level (i.e., the stability boundary) are determined as FD = 1.65 and PSE = 0.70, respectively, in this paper.

3.5 The validation of the proposed method

To verify the reliability of the proposed method, a series of acceleration signals under different milling (side milling) conditions were analyzed by the proposed method. The experimental device is the same as Sect. 3.1. The sampling frequency was set as 5120 Hz during the process of signal acquisition. The different milling experiments are labeled as no. 1, no. 2, no. 3, no. 4, no. 5, and no. 6. The cutting parameters and the analysis result of each milling state are shown in Table 4.

In Table 4, n, f_t, a_p, and w denote the spindle speed, feed per tooth, axial depth of cut, and radial depth, respectively. The surface topography of the workpiece under different milling conditions are measured by the white-light interferometer.

Fig. 16 The flow chart of online chatter monitoring strategy

As shown in Table 4, both of the surface topography of no. 1, no. 3, no. 4, and no. 5 are regular vertical texture, which conforms to the side milling mechanism, and the values of surface topography stand at relatively low values, meaning that these states are stable. According to the classification chart, almost all of the values of FD and PSE are outside of the chatter area, which are in accordance with the actual states. It is clear from Table 4 that there are two kinds of chatter, i.e., slight chatter (no. 2) and severe chatter (no. 6). Both of the surface topography of no. 2 and no. 6 are disordered, and the values of surface roughness are 1.558 and 2.867 μm, respectively, which are higher than that of under other milling conditions. In terms of the classification chart of FD and PSE, both of the values of the two indicators in no. 2 and no. 6 appear on the chatter area. Furthermore, the values of FD and PSE under no. 6 are more close to upper left corner of the classification chart, which means that the chatter condition is more severe.

To verify the advantages of the proposed method, a comparative analysis was carried out here. The standard deviation and energy ratio [27] are also used to judge the milling state. In
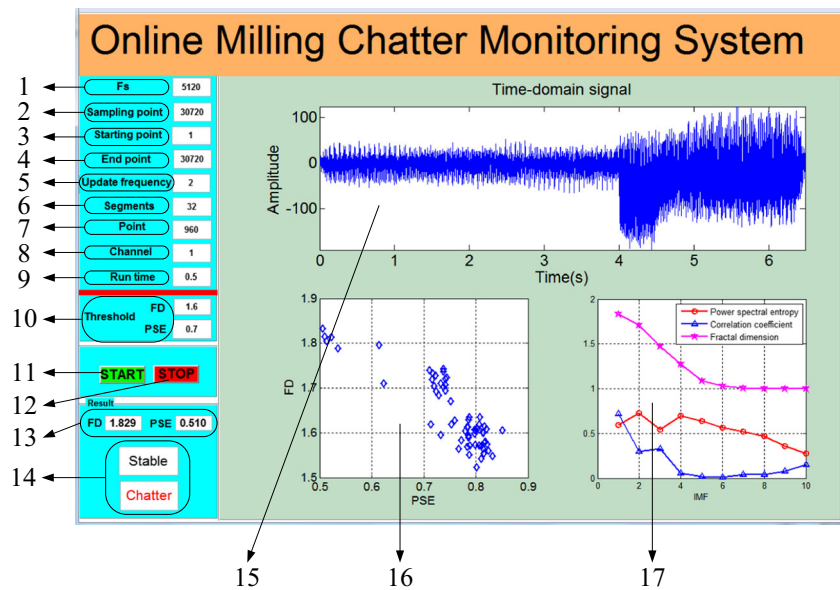

(a) The acceleration sensor

(b) The INV3062T type four channel data acquisition instrument

Fig. 17 The acceleration sensor and the signal acquisition instrument

Fig. 18 The main interface of the chatter monitoring system

this milling experiment, the axial depth of cut is set as 3 mm, feed per tooth is set as 0.02 mm, and spindle speed is set as 4000 rpm, and the radial cutting depth increases linearly from 0.5 to 2 mm; the schematic diagram is shown as Fig. 14. The experimental device is the same as Sect. 3.1. We have known that the milling process is stable (i.e., chatter-free) by detecting the signal and workpiece.

The acceleration signal and the values of FD, PSE, standard deviation (SD) and energy ratio (ER) are shown in Fig. 15. It is clear from Fig. 15 that the value of acceleration signal increases as time goes on. This is mainly due to the cutting force

increases with the increase of cutting thickness. The values of FD and PSE remain stable at approximately 1.62 and 0.80, respectively, which is consistent with the actual milling state (chatter-free). While the values of SD and ER rise gradually during the milling process. In this case, according to Liu et al. [27], chatter occurs during the milling process. But this result is not consistent with actual situation, meaning that it will cause misjudgment according to SD and ER.

Based on the above analysis, we can draw the conclusion that the proposed method is more reliable in the aspect of chatter detection.

Table 5 The details of the main interface

| Number	Functions
1	Set the sampling frequency
2	Set the sampling points
3	The starting point of the data selection
4	The end point of the data selection
5	Be used to specify how frequently the original data is refreshed
6	To determine the segment number of the original signal
7	Display the data number of each segment
8	Select the channel
9	Display the running time of signal processing
10	Set the stability boundary threshold of FD and PSE
11	Start the monitoring system
12	Stop the monitoring system
13	Real-time display the highest value of FD and the lowest value of PSE
14	Real-time display identification results (stable or chatter)
15	Real-time display the original vibration signal
16	Real-time display the distribution diagram
17	Display the fractal dimension, power spectral entropy, and correlation coefficient of each IMF

4 Online chatter monitoring strategy

Since chatter is harmful in the actual milling, and it is difficult to avoid chatter by analytical method, an online chatter monitoring strategy is proposed here. This strategy is based on the EEMD, PSE, and FD. The flow chart of this strategy is shown in Fig. 16.

The efficiency of the online chatter monitoring system greatly depends on the signal segment length. If the length of the segment is too short, the power spectral entropy cannot reflect the running state of the machine, so the data length of a segment depends on the data length of one sampling period, that is, the sampling frequency. For the purpose of obtaining an accurate result, higher sampling frequency should be set, and the number of the segments at one sampling period should depend on the actual machining state.

5 The realization of the online milling chatter monitoring

For the purpose of detecting the milling chatter timely, an online milling chatter monitoring system is developed here. The chatter monitoring system mainly consists of two parts: the hardware system and the software system. The hardware system consists of acceleration sensor (Fig. 17a), data acquisition instrument (Fig. 17b), the desktop PC, and the displayer. The acceleration sensor and the signal acquisition instrument are shown in Fig. 17. The sensitivity of the acceleration sensor is 10.355 mV/ms^2, and the available frequency range is 0.5–8000 Hz. The data acquisition instrument is an INV3062T type four-channel data acquisition instrument. The software system mainly consists of two parts: the signal processing system and state recognition system.
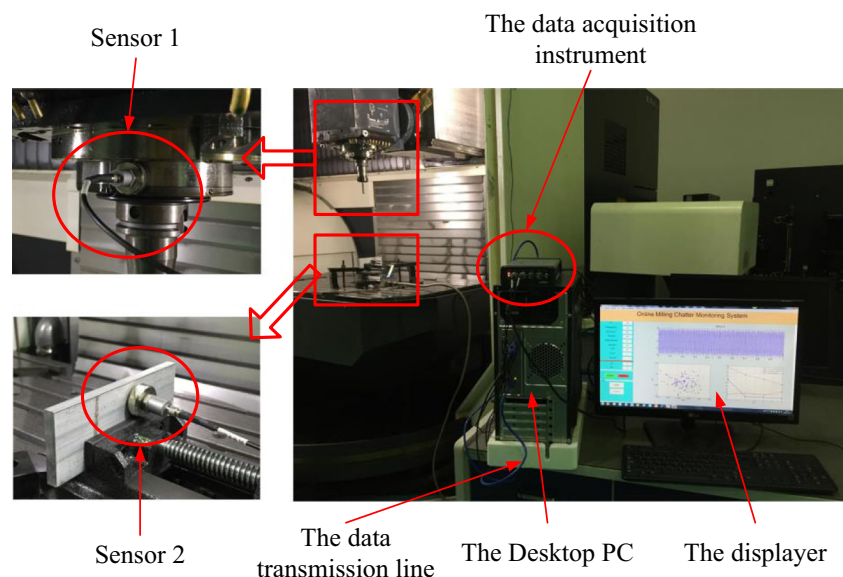
The core of this chatter monitoring system is the software system, i.e., the signal processing system and state recognition system. The software system is realized by the programming software LABVIEW 2013 and MATLAB 2012b. The functions of signal storage and real-time updates are realized by LABVIEW 2013, and the functions of signal processing and state recognition are realized by MATLAB 2012b.

The chatter recognition algorithm through software programming makes the system easy to upgrade, but also user-friendly according to their needs the flexibility to choose different recognition functions. The main interface of the chatter monitoring system is shown in Fig. 18. Table 5 shows the details of the main interface. It is very convenient to use this chatter monitoring system due to its flexible operability. The sensors can be fixed in different places according to the actual needs, and the equipment is easy to install. The practical application of the system is shown in Fig. 19.

6 Conclusions and future works

Chatter is a kind of self-excited unstable vibration during machining process, which always leads to multiple negative effects such as poor surface quality, dimension accuracy error, excessive noise, and tool wear. Online chatter monitoring is necessary in the machinery manufacturing.

A novel online chatter detection method was proposed in this article. The EEMD was applied to decompose the vibration signal into a series of IMFs. The first three IMFs which contain the most information that can reflect the running state of the machine tool were synthesized into a new signal. The new signal was divided into several segments, calculating the power spectral entropy and fractal dimension of each segment, and then the power spectral entropy curve and fractal

Fig. 19 The practical application of the online milling chatter monitoring system

dimension curve were obtained. Further, the distribution chart of the two indicators can be obtained. According to the two indicators, we can identify the milling chatter accurately. The advantages of the proposed method are described as follows:

1. The power spectral entropy can reflect the changing properties of frequency domain. In the stable milling state, the power spectral entropy reaches its maximum. Power spectral entropy will be decreased when the chatter gradually increases.

2. Fractal dimension can reflect the intrinsic properties of a signal. The fractal dimension obtained by the morphological covering method is a good nondimensional indicator for judging chatter. In the stable cutting state, the fractal dimension is fixed in a relatively small value. On the contrary, the value of fractal dimension will increase dramatically when chatter occurs.

3. The power spectral entropy and fractal dimension are combined to judge the milling state, which means that both of the frequency characteristic and morphological feature of the extracted signals can be reflected by the two indicators, so this proposed method is more reliable in the aspect of chatter detection.

In the article, a novel online milling chatter detection method was proposed, and the experiments have verified the reliability of the method. There are still some aspects need to be improved. For example, we have already realized the online monitoring here, but how to adjust the processing parameters adaptively (i.e., without human intervention) according to the monitoring information is still a challenge. On the other hand, computational efficiency is important in the aspect of condition monitoring, and the efficiency of signal processing should be improved if we want to adjust the processing parameters more quickly. These problems will be the research direction for the future works.

Reference

1. Wiercigroch M, Krivtsov AM (2001) Frictional chatter in orthogonal metal cutting. Philosophical Transactions: Mathematical Physical and Engineering Sciences (Series A) 359(1781):713–738. doi:10.1098/rsta.2000.0752

2. Wiercigroch M, Budak E (2001) Sources of nonlinearities, chatter generation and suppression in metal cutting. Philosophical Transactions of the Royal Society London 359(1781):663–693. doi:10.1098/rsta.2000.0750

3. Tlusty J, Polacek M (1963) The stability of machine tools against self-excited vibrations in machining, international research in production engineering. Mach Sci and Technol 465–474

4. Quintana G, Ciurana J (2011) Chatter in machining processes: a review. Int J Mach Tools Manuf 51(5):363–376. doi:10.1016/j.ijmachtools.2011.01.001

5. Altintas Y, Budak E (1995) Analytical prediction of stability lobes in milling. CIRP Ann Manuf Technol 44(1):357–362

6. Altintas Y (2012) Manufacturing automation: metal cutting mechanics, machine tool vibrations, and CNC design. Cambridge University Press, Cambridge

7. Gradisek J, Kalveram M, Insperger T, Weinert K, Stepan G, Govekar E, Grabec I (2005) On stability prediction for milling. Int J Mach Tools Manuf 45(7–8):769–781. doi:10.1016/j.ijmachtools.2004.11.015

8. Mann BP, Young KA, Schmitz TL, Dilley DN (2005) Simultaneous stability and surface location error predictions in milling. J Manuf Sci E-T ASME 127(3):446–453. doi:10.1115/1.1948394

9. Minis I, Yanushevsky R (1993) A new theoretical approach for the prediction of machine tool chatter in milling. J Eng Ind-Trans ASME 115(1):1–8. doi:10.1115/1.2901633

10. Budak E, Altintas Y (1998) Analytical prediction of chatter stability in milling—part I: general formulation. ASME J Dyn Syst Meas Control 120(1):22–30. doi:10.1115/1.2801317

11. Merdol SD, Altintas Y (2004) Multi frequency solution of chatter stability for low immersion milling. J Manuf Sci Eng.-Trans ASME 126(3):459–466. doi:10.1115/1.1765139

12. Altintas Y, Engin S, Budak E (1999) Analytical stability prediction and design of variable pitch cutters. J Manuf Sci Eng-Trans ASME 121(2):173–178. doi:10.1115/1.2831201

13. Altintas Y (2001) Analytical prediction of three dimensional chatter stability in milling. JSME Int J Ser C 44(3):717–723

14. Butcher EA, Ma HT, Bueler E, Averina V, Szabo Z (2004) Stability of linear time-periodic delay-differential equations via Chebyshev polynomials. Int J Numer Methods Eng 59(7):895–922. doi:10.1002/nme.894

15. Butcher EA, Bobrenkov OA, Bueler E, Nindujarla P (2009) Analysis of milling stability by the Chebyshev collocation method: algorithm and optimal stable immersion levels. J Comput Nonlinear Dyn 4(3):031003:1–03100312. doi:10.1115/1.3124088

16. Khasawneh FA, Bobrenkov OA, Mann BP, Butcher EA (2012) Investigation of period-doubling islands in milling with simultaneously engaged helical flutes. J Vib Acoust-Trans ASME 134(2):1–9. doi:10.1115/1.4 005022

17. Ding Y, Zhu LM, Zhang XJ, Ding H (2010) A full-discretization method for prediction of milling stability. Int J Mach Tools Manuf 50(5):502–509. doi:10.1016/j.ijmachtools.2010.01.003

18. Quo Q, Sun YW, Jiang Y (2012) On the accurate calculation of milling stability limits using third-order full-discretization method. Int J Mach Tools Manuf 62:61–66. doi:10.1016/j.ijmachtools.2012.05.001

19. Liu YL, Zhang DH, Wu BH (2012) An efficient full-discretization method for prediction of milling stability. Int J Mach Tools Manuf 63:44–48. doi:10.1016/j.ijmachtools.2012.07.008

20. Abellan-Nebot JV, Subirón FR (2010) A review of machining monitoring systems based on artificial intelligence process models. Int J Adv Manuf Technol 47(1–4):237–257. doi:10.1007/s00170-009-2191-8

21. Lamraoui M, Thomas M, El Badaoui M, Girardin F (2014a) Indicators for monitoring chatter in milling based on instantaneous angular speeds. Mech Syst Signal Proc 44(1–2):72–85. doi:10.1016/j.ymssp.2013.05.002

22. Lamraoui M, Thomas M, El Badaoui M (2014b) Cyclostationarity approach for monitoring chatter and tool wear in high speed milling. Mech Syst Signal Proc 44(1–2):177–198. doi:10.1016/j.ymssp.2013.05.001

23. Thaler T, Potočnik P, Bric I, Govekar E (2014) Chatter detection in band sawing based on discriminant analysis of sound features. Appl Acoust 77:114–121. doi:10.1016/j.apacoust.2012.12.004

24. Huang PL, Li JF, Sun J, Zhou J (2013) Vibration analysis in milling titanium alloy based on signal processing of cutting force. Int J Adv Manuf Technol 64(5–8):613–621. doi:10.1007/s00170-012-4039-x

25. Tangjitsitcharoen S, Pongsathornwiwat N (2013) Development of chatter detection in milling processes. Int J Adv Manuf Technol 65(5–8):919–927. doi:10.1007/s00170-012-4228-7

26. Tansel IN, Li M, Demetgul M, Bickraj K, Kaya B, Ozcelik B (2012) Detecting chatter and estimating wear from the torque of end milling signals by using Index Based Reasoner (IBR). Int J Adv Manuf Technol 58(1–4):109–118. doi:10.1007/s00170-010-2838-5

27. Liu Y, Wang XF, Lin J, Zhao W (2016) Early chatter detection in gear grinding process using servo feed motor current. Int J Adv Manuf Technol 83(9–12):1801–1810. doi:10.1007/s00170-015-7687-9

28. Weng JW, Zhong JG (2003) Application of Gabor transform to 3-D shape analysis. Acta Photonica Sinica 32(08):993–996

29. Postnikov EB, Lebedeva EA, Lavrova AI (2016) Computational implementation of the inverse continuous wavelet transform without a requirement of the admissibility condition. Appl Math Comput 282:128–136. doi:10.1016/j.amc.2016.02.013

30. Staszewski WJ, Worden K, Tomlinson GR (1997) Time-frequency analysis in gearbox fault detection using the Wigner-Ville distribution and pattern recognition. Mech Syst Signal Proc 11(5):673–692. doi:10.1006/mssp.1997.0102

31. Pachori RB, Nishad A (2016) Cross-terms reduction in the Wigner-Ville distribution using tunable-Q wavelet transform. Signal Process 120:288–304. doi:10.1016/j.sigpro.2015.07.026

32. Fu Y, Zhang Y, Zhou HM, Li DQ, Liu HQ, Qiao HY, Wang XQ (2016) Timely online chatter detection in end milling process. Mech Syst Signal Proc 75:668–688. doi:10.1016/j.ymssp.2016.01.003

33. Huang NE, Shen Z, Long SR, Wu MC, Shih HH, Zheng QA, Yen NC, Tung CC, Liu HH (1998) The empirical mode decomposition and the Hilbert spectrum for nonlinear non-stationary time series analysis. Proc R Soc Lond A 454:903–995

34. Huang NE, Wu ZH (2008) A review on Hilbert-Huang transform: method and its applications to geophysical studies. Rev Geophys 46(2):1–23. doi:10.1029/2007RG000228

35. Wu ZH, Huang NE (2009) Ensemble empirical mode decomposition: a noise assisted data analysis method. Adv Adapt Data Anal 1(1):1–41. doi:10.1142/S1793536909000047

36. Liu H, Tian HQ, Liang XF, Li YF (2015) New wind speed forecasting approaches using fast ensemble empirical model decomposition, genetic algorithm, mind evolutionary algorithm and artificial neural networks. Renew Energy 83:1066–1075. doi:10.1016/j.renene.2015.06.004

37. Wang SX, Zhang N, Wu L, Wang YM (2016) Wind speed forecasting based on the hybrid ensemble empirical mode decomposition and GA-BP neural network method. Renew Energy 94:629–636. doi:10.1016/j.renene.2016.03.103

38. Xian L, He KJ, Lai KK (2016) Gold price analysis based on ensemble empirical model decomposition and independent component analysis. Physica A 454:11–23. doi:10.1016/j.physa.2016.02.055

39. Yang CY, Wu TY (2015) Diagnostics of gear deterioration using EEMD approach and PCA process. Measurement 61:75–87. doi:10.1016/j.measurement.2014.10.026

40. Tabrizi A, Garibaldi L, Fasana A, Marchesiello S (2015) Early damage detection of roller bearings using wavelet packet decomposition, ensemble empirical mode decomposition and support vector machine. Meccanica 50(3):865–874. doi:10.1007/s11012-014-9968-z

41. Žvokelj M, Zupan S, Prebil I (2016) EEMD-based multiscale ICA method for slewing bearing fault detection and diagnosis. J Sound Vibr 370:394–423. doi:10.1016/j.jsv.2016.01.046

42. Xu J, Wang ZB, Tan C, Si L, Liu XH (2015) A cutting pattern recognition method for shearers based on improved ensemble empirical mode decomposition and a probabilistic neural network. Sensors 15(11):27721–27737. doi:10.3390/s151127721

43. Siddhpura M, Paurobally R (2012) A review of chatter vibration research in turning. Int J Mach Tools Manuf 61:27–47. doi:10.1016/j.ijmachtools.2012.05.007

44. Gray RM (2009) Entropy and information theory. Springer-Verlag, New York

45. Mandelbrot BB (1982) The fractal geometry of nature. Freeman, New York

46. Mandelbrot BB (2006) Fractal analysis and synthesis of fracture surface roughness and related forms of complexity and disorder. Int J Fract 138(1–4):13–17. doi:10.1007/s10704-006-0037-z

47. Bramowicz M, Braic L, Azem FA, Kulesza S, Birlik I (2016) Mechanical properties and fractal analysis of the surface texture of sputtered hydroxyapatite coatings. Appl Surf Sci 379:338–346. doi:10.1016/j.Apsusc.2016.04.077

48. Liu SC, Chang S (1997) Dimension estimation of discrete-time fractional Brownian motion with applications to image texture classification. IEEE Trans Image Process 6(8):1176–1184. doi:10.1109/83.605414

49. Neil G, Curtis KM (1997) Shape recognition using fractal geometry. Pattern Recogn 30(12):1957–1969. doi:10.1016/S0031-3203(96)00193-8

50. Lin KH, Lam KM, Siu WC (2001) Locating the eye in human face images using fractal dimensions. IEE Proc-Vis Image Signal Process 148(6):413–421. doi:10.1049/ip-vis:20010709

51. Sarker N, Chaudhuri BB (1994) An efficient differential box-counting approach to compute fractal dimension of image. IEEE Transactions on Systems, Man, and Cybernetics 24(1):115–120. doi:10.1109/21.259692

52. Maragos P, Sun FK (1993) Measuring the fractal dimension of signals: morphological covers and iterative optimization. IEEE Trans Signal Process 41(1):108–121. doi:10.1109/TSP.1993.193131

53. Cao HR, Zhou K, Ghen XF (2015) Chatter identification in end milling process based on EEMD and nonlinear dimensionless indicators. Int J Mach Tools Manuf 92:52–59. doi:10.1016/j.ijmachtools.2015.03.002

54. Shen JL, Hung JW, Lee LS (1998) Robust entropy-based end point detection for speech recognition in noisy environments. in: The International Conference on Spoken Language Processing, Incorporating the Australian International Speech Science and Technology Conference, Sydney Convention Centre, Sydney, Australia, November-December. DBLP 232–235

55. Insperger T, Stépán G (2004) Updated semi-discretization method for periodic delay- differential equations with discrete delay. Int J Numer Methods Eng 61(1):117–141. doi:10.1002/nme.1061

56. Xun J, Yan SZ (2008) A revised Hilbert-Huang transformation based on the neural networks and its application in vibration signal analysis of a deployable structure. Mech Syst Signal Proc 22(7):1705–1723. doi:10.1016/j.ymssp.2008.02.008

57. Insperger T, Stépán G, Bayly PV, Mann BP (2003) Multiple chatter frequencies in milling processes. J Sound Vib 262(2):333–345. doi:10.1016/S0022-460X(02)01131-8

58. Feng JL, Sun ZL, Jiang ZH, Yang L (2016) Identification of chatter in milling of Ti-6Al-4V titanium alloy thin-walled workpieces based on cutting force signals and surface topography. Int J Adv Manuf Technol 82(9–12):1909–1920. doi:10.1007/s00170-015-7509-0

The main codes for computing the fractal dimension (obtained by the morphological covering method) are given in the appendices in order to provide a full understanding of the method. These codes are inspired by reference [52] and Jesús Monge-Álvarez, University of Valladolid. The original codes are available on the website: https://cn.mathworks.com/matlabcentral/fileexchange/51175-margaos-sun-fractal-dimension